Light extinction at agglomerates of spheres-A practical test on the submicroscale

Uwe Kätzel, Frédéric Gruy, Frank Babick, Wolfgang Klöden

Light Extinction at Agglomerates of Spheres – A practical test on the sub-microscale

Uwe Kätzel[*], Frederic Gruy[**], Frank Babick[*], Wolfgang Klöden[*]

Received:

[*] Dipl.-Ing. U. Kätzel, Dipl.-Ing. F. Babick, Prof. W. Klöden, Institut für Verfahrenstechnik und Umwelttechnik, TU Dresden, Münchner Platz 3, 01062 Dresden, Germany

[**] Prof. F. Gruy, Centre SPIN, Ecole Nationale Supérieure des Mines, 158 Cours Fauriel, 42023 St. Etienne, France, to whom correspondence should be addressed

email : gruy@emse.fr

Abstract

Today's theories applied for the inversion of measurement data from optical measurement devices are restricted to single spherical particles. However, particles formed in industrial processes like precipitation and crystallization are often non-spherical or agglomerates. Theoretical approaches to describe the optical behavior of such particle systems have already been proposed. The verification of these theories has mostly been done using microwave scattering experiments with agglomerates in the millimeter range. This paper provides a first but surely not all-embracing practical test for a general extension of the Mie theory to agglomerates of sub-microscale spheres. For the sake of simplicity and from practical viewpoints of the online-sensor development only light extinction of an agglomerated suspension has been examined. The required rigid agglomerates have been produced using a spray-drying method that generates particles with a much higher mechanical stability than can be obtained by usual procedures. Subsequent fractionation of the suspension delivers systems with only a limited number of agglomerate configurations. Extinction measurements at multiple wavelengths using Dynamic Extinction Spectroscopy have been conducted for the determination of the extinction cross section of the agglomerated dispersions. These data are compared with agglomerate scattering computations.

Keywords: light extinction, Mie theory, agglomerates, dynamic extinction spectrosocopy

1 Introduction

Optical measurement techniques to characterize the particle size or particle concentration are widely used in industrial applications. Online or inline setups for sensors are mostly based on light extinction or backscattering. To extract information about a particle size distribution multiple wavelengths or multiple angles are used [1-3]. Such sensor systems are typically employed in precipitation and crystallization processes because the final particle size of the product essentially controls the system properties. The advantage of optical devices for particle sizing is their simple and robust sensor setup and their relatively low sensitivity to material properties. On the other hand the interpretation of the optical signals requires inversion procedures based on a theoretical relationship between size and optical behavior of the particles.

Over many years the Mie theory [4-7] has become the most widely used model when the particle size of the observed systems is in the range of the wavelength of the light beam. The applicability of this theory is restricted to single homogeneous spheres with no contact to neighbouring particles. However, particles formed by precipitation and crystallization are often non-spherical or agglomerates. Therefore approaches for a more general model, that considers the influence of particle shape and agglomerate structure were early developed [8-12].

In general, there are two areas of interest that have been examined in the past years. The first is the scattering behavior of non-spherical particles. It can be solved e.g. by using the T-Matrix approach or the Multiple Multipole technique [13-20]. The second area is the scattering of agglomerates, that is of relevance in particle science, chemistry, meteorology and astronomy. Development here started also early with the pioneering works of Bruning and Lo [21-23] and was extended by Fuller and Kattawar [24,25] and Mackowski [26]. Xu [27-29] summarized these previous approaches and presented a fully analytical solution for agglomerates of spheres, which is closely related to the Mie theory. The combination of Xu's approach with the T-Matrix calculation by Xu and Khlebtsov [30] enables the theoretical computation of the light scattering behavior of agglomerates of arbitrarily shaped scatterers. The experimental verification of these theories has been done by using ideal agglomerates of millimeter size in microwave scattering facilities, so there is no doubt about the principal validity of the scattering theories. However, the application in optical measurement devices for the observation of agglomerates in industrial processes involves practical problems that are due to the measurement device itself such as the laser intensity profile in the measurement volume, intensity fluctuations, nonideal detectors and data processing or to the systems under study due to impurities, gas bubbles, changes in re-

fractive index or particle shape. It might be very easy to obtain scattering data in such applications but it is still challenging whether these data can be related to results from multisphere scattering theories.

The objective of this paper is to present a first test of the aforementioned approach of Xu for agglomerates of spheres in systems in the sub-microscale by means of extinction measurements. Measured extinction coefficients of suspensions of known composition have been compared to the prediction of the theory, the inverse problem of relating the measured extinction coefficients in suspensions of unknown composition to agglomerate sizes are not in the scope of this paper. Special attention will be paid to agglomerates with a small number of primary particles because of their high occurrence in stirred precipitation reactors. After a short review of the principle of the theory extension in the next section a method to produce rigid agglomerates in the submicrometer range will be presented in section 3. This is necessary, because the agglomerate configurations shall firstly not change during the test experiments. One notice that rigid agglomerates are mainly produced in all precipitation reactors by particles collision followed by crystal growth at the neck of the two-particle set. Subsequently, a fractionation method to reach suspensions of just a few different agglomerates will be discussed briefly in section 4. Section 5 is devoted to the extinction measurements that have been carried out for comparison. This measurement principle has been chosen because it is often used for process monitoring in industrial processes of precipitation and crystallization. Section 6 presents the results of the test experiments.

2 Theory

The concept of the extension of the Mie theory to agglomerates of spheres is straightforward. As long as the primary particles do not intersect, it is possible to apply the solution of the time-harmonic vector wave equations for the electric and the magnetic field independently due to the continuous boundary. That means the result must be an infinite series expansion of the two spherical vector wave functions in spherical coordinates [27].

$$\mathbf{M}_{mn}^{(J)} = \left[\mathbf{i}_\theta \, \mathrm{i}\, \pi_{mn}(\cos\theta) - \mathbf{i}_\phi \, \tau_{mn}(\cos\theta)\right] z_n^{(J)}(k\,r) \exp(\mathrm{i}\, m\,\phi) \tag{1}$$

$$\begin{aligned}\mathbf{N}_{mn}^{(J)} = {} & \mathbf{i}_r \, n(n+1)\, \mathrm{P}_n^m(\cos\theta) \frac{z_n^{(J)}(k\,r)}{k\,r} \exp(\mathrm{i}\, m\,\phi) \\ & + \left[\mathbf{i}_\theta \tau_{mn}(\cos\theta) + \mathbf{i}_\phi \, \mathrm{i}\, \pi_{mn}(\cos\theta)\right] \frac{1}{k\,r} \frac{d}{d\,r} \left[r\, z_n^{(J)}(k\,r)\right] \exp(\mathrm{i}\, m\,\phi)\end{aligned} \tag{2}$$

where **i** is the unit vector in the coordinate system, i is the imaginary unit $\sqrt{-1}$, π_{mn} and τ_{mn} are the Mie angular functions as defined in Appendix A, $z_n^{(J)}$ is one of the four spherical Bessel functions of kind

J and order n, P_n^m is the associated Legendre Polynomial and k is the wave number. The incident, scattered and internal electric field of the j-th sphere can then be expanded as follows:

$$\mathbf{E}_{inc}(j) = -\sum_{n=1}^{\infty}\sum_{m=-n}^{n} \mathrm{i}\, E_{mn}\left[p_{mn}^{j}\,\mathbf{N}_{mn}^{(1)} + q_{mn}^{j}\,\mathbf{M}_{mn}^{(1)}\right] \tag{3}$$

$$\mathbf{E}_{sca}(j) = \sum_{n=1}^{\infty}\sum_{m=-n}^{n} \mathrm{i}\, E_{mn}\left[a_{mn}^{j}\,\mathbf{N}_{mn}^{(3)} + b_{mn}^{j}\,\mathbf{M}_{mn}^{(3)}\right] \tag{4}$$

$$\mathbf{E}_{int}(j) = -\sum_{n=1}^{\infty}\sum_{m=-n}^{n} \mathrm{i}\, E_{mn}\left[d_{mn}^{j}\,\mathbf{N}_{mn}^{(1)} + c_{mn}^{j}\,\mathbf{M}_{mn}^{(1)}\right] \tag{5}$$

The superscript $^{(1)}$ defines the generating function to be the spherical Bessel function of the first kind while the superscript $^{(3)}$ designates the spherical Hankel function of the first kind. The formulations for the magnetic fields are similar. E_{mn} is a normalization factor that can be found in Appendix A. Xu [27] has shown that the expansion coefficients for the three different fields can be linked by the known Mie coefficients a_n and b_n for single-sphere scattering:

$$a_{mn}^{j} = a_n^{j}\; p_{mn}^{j} \quad b_{mn}^{j} = b_n^{j}\; q_{mn}^{j} \tag{6}$$

$$c_{mn}^{j} = c_n^{j}\; q_{mn}^{j} \quad d_{mn}^{j} = d_n^{j}\; p_{mn}^{j} \tag{7}$$

That means, for a correct solution of the scattering behavior of an arbitrary sphere only the profile of the incident beam must be known in terms of the expansion coefficients p and q. They have to contain the original impinging wave and the scattered waves from all the other spheres.

The calculation of this profile then includes the transformation of the scattered field of one sphere in the coordinate system of another particle. This can be done by using translation theorems for vector fields as described by Cruzan [31]. Finally, a large system of linear equations for the calculation of the partial scattering coefficients a_{mn}^{j} and b_{mn}^{j} has to be solved:

$$a_{mn}^{j} = a_n^{j}\left[p_{mn}^{j} - \sum_{l\neq j}^{[1,N_{prim}]}\sum_{n=1}^{\infty}\sum_{m=-n}^{n}\left(a_{\mu\nu}^{l}\,A_{mn\mu\nu}^{lj} + b_{\mu\nu}^{l}\,B_{mn\mu\nu}^{lj}\right)\right] \tag{8}$$

$$b_{mn}^{j} = b_n^{j}\left[q_{mn}^{j} - \sum_{l\neq j}^{[1,N_{prim}]}\sum_{n=1}^{\infty}\sum_{m=-n}^{n}\left(a_{\mu\nu}^{l}\,B_{mn\mu\nu}^{lj} + b_{\mu\nu}^{l}\,A_{mn\mu\nu}^{lj}\right)\right] \tag{9}$$

where A and B are so-called vector translation coefficients introduced by Cruzan. Formulations can also be found in Xu [32]. The criterion of Wiscombe [33] can be used for series cut in dependence on the size parameter of the primary spheres α_l.

$$N_w^l = \alpha_l + 4\alpha_l^{1/3} + 2 \tag{10}$$

There are two assumptions about the geometry of the system involved in this derivation. The light that impinges on the particle agglomerate is supposed to travel in the positive z-direction and the detector shall be situated far from the observed ensemble. This is equipollent with the far-field approximation in the Mie theory as discussed by Kerker [6]. With these assumptions, explicit formulations for the expansion coefficients of the incident field may be found [34]. After the solution of the system of linear equations, the cross sections for extinction and scattering can be derived using the partial scattering coefficients a_{mn}^j and b_{mn}^j:

$$C_{ext} = \sum_{l=1}^{N_{prim}} C_{ext}^l = \frac{4\pi}{k^2} \sum_{l=1}^{N_{prim}} \sum_{n=1}^{N_w^l} \sum_{m=-n}^{n} \mathrm{Re}\left(p_{mn}^{l*}\, a_{mn}^l + q_{mn}^{l*}\, b_{mn}^l \right) \tag{11}$$

$$C_{sca} = \sum_{l=1}^{N_{prim}} C_{sca}^l = \frac{4\pi}{k^2} \sum_{l=1}^{N_{prim}} \sum_{n=1}^{N_w^l} \sum_{m=-n}^{n} \mathrm{Re}\left(a_{mn}^{l*}\, a_{mn}^{(l)} + b_{mn}^{l*}\, b_{mn}^{(l)} \right) \tag{12}$$

where

$$a_{mn}^{(l)} = \sum_{j=1}^{N_{prim}} \sum_{\nu=1}^{N_w^l} \sum_{\mu=-\nu}^{\nu} \left(\tilde{A}_{mn\mu\nu}^{lj}\, a_{\mu\nu}^j + \tilde{B}_{mn\mu\nu}^{lj}\, b_{\mu\nu}^j \right) \tag{13}$$

$$b_{mn}^{(l)} = \sum_{j=1}^{N_{prim}} \sum_{\nu=1}^{N_w^l} \sum_{\mu=-\nu}^{\nu} \left(\tilde{B}_{mn\mu\nu}^{lj}\, a_{\mu\nu}^j + \tilde{A}_{mn\mu\nu}^{lj}\, b_{\mu\nu}^j \right) \tag{14}$$

The asterisk denotes complex conjugate values. The vector translation coefficients in Eq. [13,14] have been marked with a tilde to distinguish them from the values given in Eq. [8,9]. The spherical Hankel function of the first kind is the generating function of the former coefficients while the spherical Bessel function of the first kind is used for the latter ones. The similarity of the obtained equations to the ones derived in the Mie theory is obvious. They reduce exactly to the same form when an agglomerate consists of only one sphere.

Another problem, which does not occur in single sphere scattering, is the dependence of the optical behavior on the orientation of the particle ensemble to the light beam. For particles in suspensions or aerosols where no preferential orientation exists, one needs averaged values. There are two different approaches to deal with this problem. The first is the use of the T-Matrix approach [30], which enlarges memory consumption of the computation, and the second one is discrete orientation-averaging, which enlarges computation time. Thus, the theory enables the calculation of scattering properties of agglomerates in suspensions if the composition of the suspension and the exact spatial configuration

of primary particles in the agglomerates as well as the optical properties of the primary particles are known.

One theoretical test to prove the correctness of the framework can be done as follows.. When increasing the center to center separation in a two-sphere chain arranged on the y-axis, one has to reach the Mie solution at large distances. Two examples are given in Figure 1. The left figure handles spheres of size parameter α=6.613; 5.290; 3.306 while the right diagram shows the values for α=0.661; 0.331; 0.066 over the dimensionless separation distance *kd*. The refractive index was kept constant at 1.57-0i. For simplicity only the deviations from the Mie theory for the extinction cross section have been displayed. The incident wave has been chosen to be x-polarized which is equipollent with a polarization angle of 0°.

Figure 1

It can be seen that for the doublets of large primary particles the interactions are not very strong (maximum deviation about 7 %) and that they decay quite fast. Already at a distance of only one sphere diameter the multisphere interactions are negligible. This observation does not hold for very small primary particles. Deviations are much higher here. Additionally a certain interference between the fields of the two scattering dipoles appears at a separation distance of *kd*=8. That means multiparticle interactions for Rayleigh scatterers can only be neglected for very low concentrations.

Of course this theoretical test is not sufficient to prove the correctness of the theory. Therefore Xu and Gustafson [34,35] have conducted many microwave scattering experiments using very different sphere configurations. The agreement of the experimental results with the computations was always impressive.

3 Experimental

3.1 Production of rigid agglomerates

Experiments to test theories for agglomerate scattering require some specific properties of the particle systems. Firstly, the primary particles need to be spheres with known size and refractive index. Secondly, the produced agglomerates must not change size or configuration during an experiment otherwise an exact theoretical prediction is nearly impossible. Two silica powders (Geltech 500 and Geltech 1000) have been selected for these experiments. They provide monodisperse spherical particles of 580 nm and 800 nm diameter, respectively. Their refractive index has been determined using embed-

ding methods with an index-matching fluid and extinction measurements. The indices are summarized in Table 1.

Table 1

Different procedures have been tested for agglomerate production. The first approach was to use usual agglomeration procedures by changing the electric charge distribution on the surface of the particles. The resulting agglomerates are usually in a dynamic equilibrium that depends on external influences such as the stirrer speed. To introduce rigidity one has to stabilize the agglomerates when the desired configurations predominate in the suspension. This can be done by precipitation of a small amount of salt, where the particles serve as crystallization nuclei. Precipitation by temperature change will introduce kinetic problems. Therefore a salt-out procedure, which is the crystallization of the salt by addition of a second solvent in which the salt is not soluble, has been used. The solvents were water and ethanol while potassium sulfate was used for precipitation. The resulting agglomerates are stable but cannot be controlled in size due to surface processes on the silica particles. Therefore this method has to be discarded.

Secondly, a suspension dryer (Büchi Mini Spray Dryer B191, Büchi AG) was used. The primary particles are sprayed in a hot drying zone of about 200 °C, where the agglomerates are formed by evaporation. They are subsequently separated in a cyclone. The gained agglomerates are nearly spherical as can be seen in figure 2.

Figure 2

However, the examination of the mechanical stability revealed that the agglomerates are breakable by very low mechanical stress. That means, they cannot be fractionated by filtration or centrifugation which is necessary to not have a too high amount of different agglomerate configurations in the subsequent experiments. This is due to the very fast drying procedure where only weak bonds between the primary particles can be established.

Eventually, stable agglomerates were obtained by the Aerosol Resuspension Method. The suspensions containing the primary particles are given to an aerosol generator and sprayed with compressed air. The principle of operation is an injector. The mean drop size is about 5 µm. The droplets are subse-

quently dried in a glass tube at room temperature of about 25 °C. Therefore a cladding flow of dry air is added. Finally the agglomerates are directly resuspended in water and stabilized by adjusting the pH to a value of 9 through the addition of potassium hydroxide. The recovery rate has been optimized using a bubble breaker in the resuspension reservoir so a final concentration of agglomerates of about 1 vol.-% could be gained. A scheme of the arrangement is given in figure 3.

Figure 3

The mean number of particles in the droplets can be directly influenced by the feed concentration. This in turn affects agglomerate sizes and configurations, as is shown in figure 4 for 2 samples with different feed concentrations. For the use in these practical tests, firstly agglomerates with a small number of primary particles are preferred due to less computation effort and of course due to their importance in precipitation and crystallization experiments. Therefore the concentrations of the suspensions have been calculated for only three silica spheres per droplet in average, which are 0.468 vol.-% for Geltech 500 and 1.229 vol.-% for Geltech 1000.

Figure 4

The main differences to the Spray Dryer are the size of the droplets and the temperature in the drying section. For this reason the stability of the gained agglomerate suspensions was subsequently examined, too. The particle size distribution can clearly show whether coarse particle fractions or agglomerates in this special case are destroyed by mechanical treatment such as stirring or sonification. Size distributions of the samples have been directly measured after spraying and resuspension. Laser diffraction (HELOS, Sympatec GmbH) is the most feasible technique due to the fast and robust measurements. By sonification with a device-integrated actuator (Power: 30 W) and a US-desintegrator (200 W) the samples were exerted to mechanical stress of different intensity. Figure 5 presents the volume density distributions for Geltech 500.

Figure 5

The stability of this suspension is high compared to the Spray Dryer agglomerates probably due to the temperature difference during drying. It has to be noted that the stability again decreases with bigger primary particles or smaller agglomerate sizes. That is for suspensions sprayed with low concentrations due to the smaller number of contact points of the spheres. However, the gained suspensions will not be changed during fractionation and extinction measurements.

3.2 Fractionation

The need for a fractionation is clearly visible from figure 4. Though the drop size distribution of the selected aerosol generator is quite narrow also stochastic distribution of the primary particles in the droplets lead to a large variety of different agglomerate configurations. As the utilized program only calculates one agglomerate in a run, this would lead to enormous computations for the comparison. So the goal is to reach suspensions of just a few different configurations. In principle there are two methods for fractionation, filtration and centrifugation. The use of a centrifugation method has been preferred in this work due to the significant difference in settling velocity between the desired agglomerates. Additionally the use of a photo-centrifuge enables direct observation of the fractionation process. The exact method has been described elsewhere [36]. Firstly the amount of primary particles has been reduced by stopping the centrifugation just after all desired agglomerates settled and removing the supernatant several times. Afterwards the same cut has been done between the doublets and triplets of silica to reach a suspension that has a large amount of doublets. Table 2 lists the relative occurrence of the agglomerate suspensions after the fractionation process obtained by counting of SEM pictures for Geltech 500 and Geltech 1000. A number of 20 SEM pictures and about 200 particles and agglomerates have been considered representative for each suspension. Figure 6 gives an overview of the different agglomerate morphologies found in the images.

Table 2

Figure 6

The amount of primary particles is still considerably high which will effect the differences in optical particle characterization. On the other hand it is not possible at the moment to further reduce this content because the difference in sedimentation velocity is not big enough. One would have to change

either the viscosity of the suspension medium to get a higher settling time difference but this is counteracted by the problem of resuspending the particles in the medium after spraying. Another possible improvement would be to use line start centrifugation because then all doublets will reach the sediment at the same time and the fractionation will be much sharper. Contrariwise the dilution of the sample will be very high in this case so subsequent concentration procedures have to be established after every fractionation step. Therefore the present fractionation samples have been used for the extinction measurements. Significant changes in measurement signals compared to a suspension containing only primary particles can, however, be expected.

3.3 Extinction Measurements

One optical property that can be measured easily is the extinction cross section. When measuring the transmission, i.e. the ratio of the intensity of a light beam after passing a sample suspension to the incident intensity, one only needs Lambert-Beer's law for low concentrations to gain the extinction cross section:

$$T = \frac{I}{I_0};\ E = -\ln\ T = C_{ext}\, l_p\, c_N \tag{15}$$

where T is the transmission, I the intensity, E the extinction, l_p the optical path length, i.e. the way that the light travels through the sample, and c_N the number volume concentration of the particles in the examined system. The determination of this concentration is also very important in the tests with agglomerate suspensions. The concentrations of the fractionated suspensions are summarized in Table 3:

Table 3

Because of this easy and robust assembly, measurements of the suspensions transmission are highly favorable for online or inline metrology. Dynamic extinction spectroscopy is the combination of dynamic extinction measurements and extinction spectroscopy. Dynamic extinction means the measurement of the mean transmission of a sample as well as the standard deviation of the transmission. Extinction cross section and concentration can be calculated from these two values. Extinction spectroscopy means the simultaneous measurement of the transmission at multiple wavelengths. The combination of the two methods can cover a wide spectrum of particle sizes. The principle and theoretical

background can be found in [1,37]. The used device was an AELLO 1400 (AELLO c/o GWT TU Dresden GmbH). The extinction spectroscopy mode enables the measurement of transmission data at three different wavelengths (470 nm, 670 nm, 875 nm). Advantageous is the small aperture angle of the device which does not change much the measured extinction values. As both silica samples show a significant change in complex refractive index when measuring in the UV range, only the wavelengths in the red and infrared range were used.

4 Results and Discussion

As already shown in Table 2 the agglomerate suspensions consist of different agglomerate configurations. For each of these ensembles the orientation-averaged extinction cross section was calculated with a program using Xu's extension of the Mie theory for both wavelengths of the Dynamic Extinction Spectrometer AELLO 1400. The refractive index of the suspension medium in the calculation was 1.330 (670 nm) and 1.326 (875 nm), respectively. As the volume concentrations cannot be directly converted to number volume concentrations for a distribution of agglomerates, the volume specific extinction cross section has to be calculated for each sphere ensemble using the following equation:

$$C_{V,ext} = \frac{3}{2\,x_V} Q_{ext} \tag{16}$$

Here, Q_{ext} is the extinction efficiency and x_V is the particle size of the volume-equivalent sphere. By substituting Q_{ext} and by assuming that the agglomerate consists of primary particles of the same size one yields a direct expression.

$$C_{V,ext,agg} = \frac{6}{N_{prim}\,\pi\,x_{prim}^{\,3}} C_{ext,agg} \tag{17}$$

The extinction coefficient of the agglomerate suspensions was measured 50 times for each concentration using the Aello 1400 in a stirred beaker. The deviation of the mean transmission value was always smaller than 1 % so the reproducibility of the measurements was very good.

The calculated cross sections and the measured cross sections are finally compared in Table 4. Additionally computed values for the volume specific extinction cross sections for suspensions that contain only the primary particles instead of agglomerates are given in the table for comparison.

Table 4

At first sight the deviations between the computed results for the primary particles and the agglomerate suspension are not very high, so one could doubt about the significance in changes of the measurement data. However, the measurement error has always been smaller than this difference, so the deviation clearly stems from the agglomerates present in the suspension rather than from measurement errors. A principal error in the measurement could be the finite aperture of the device which would result in a smaller extinction cross section because forward scattered light is additionally collected on the detector. As already mentioned the aperture angle of the detector of the AELLO 1400 is quite small and as can be seen from Table 4 the measured cross section are almost higher than the theoretical predictions. This probably is due to a higher amount of agglomerates present in the suspension than counted from the SEM pictures. They could have been broken up by the stress of the sample preparation for the SEM so they were erroneously counted as primary particles. Another possible error arising from these measurements are uncertainties in the concentration measurement. The higher deviations between computed and measured data for Geltech 500 are due to a higher uncertainty in the volume concentration. However, it can be stated that the values agree within acceptable errors. This clearly underlines the possibilities of the application of aggregate scattering calculations as for the analysis of scattering or extinction data in online metrology of particle sizes. . Further test experiments should especially pay attention to the exact determination of the volume concentration of the agglomerate suspension, the fractionation process and the knowledge of the complex refractive index of the particulate matter.

5 Conclusions

Agglomerates of spherical particles involve practical problems in the interpretation of measurement signals from optical particle measurement devices due to the interactions of the scattered fields of neighboring particles that are not taken into account by the commonly used Mie theory. However several theoretical approaches to account for agglomerated structures of spheres are known. In this paper the extension of Xu was used. Sub-microscale systems under study for the test experiments require rigid agglomerates. These can be produced using the Aerosol Resuspension Method. The size of the ensembles can be adjusted by the feed concentration in the aerosol generator. The stability of the gained agglomerates was verified using established Laser Diffraction measurements. Centrifugation was used to concentrate the desired agglomerate configurations. Still, improvements might provide better results especially for the separation of the primary particles. Dynamic Extinction Spectros-

copy was used to measure the extinction cross sections of the examined systems at multiple wavelengths. Finally, the measured values show a good agreement with the extinction cross sections calculated with a program, that contains Xu's algorithms. Another important point of the application of these theories to the analysis of online data is that the according computations have to be quite fast. This is nowadays still a drawback of all available methods that overcome the limitations of the Mie theory. However, with the background of the test experiments one can address the applicability of approximate methods for aggregate scattering such as the methods presented by Gruy [38]. This work is actually carried out and will be published in another paper.

6 Acknowledgements

The authors express their gratitude to the *Ernest-Solvay-Foundation* for its financial support.

7 Appendix A

The Mie angular functions π_{mn} and τ_{mn} are defined as:

$$\pi_{mn}(\cos\theta) = \frac{m}{\sin\theta} \mathrm{P}_n^m(\cos\theta) \tag{A1}$$

$$\tau_{mn}(\cos\theta) = \frac{d}{d\theta} \mathrm{P}_n^m(\cos\theta) \tag{A2}$$

where n and m are integers with $n > 0$, $-n \geq m \geq n$ and P_n^m is the associated Legendre polynomial.

The extensions of the electric and magnetic field are normalized with a factor E_{mn} to keep the formulations in agreement with the Mie theory when dealing with only one sphere in an agglomerate. Xu uses two different formulations so one has to take care for all following equations especially for the vector translation coefficients, which are changed likewise:

Formulation in [3,4,5,8]:

$$E_{mn} = |E_0| \mathrm{i}^n (2n+1) \frac{(n-m)!}{(n+m)!} \tag{A3}$$

Formulation in [6]:

$$E_{mn} = |E_0| \mathrm{i}^n \left[\frac{(2n+1)(n-m)!}{n(n+1)(n+m)!} \right]^{1/2} \tag{A4}$$

8 Symbols

a_n	Mie coefficient
a_{mn}^j	Partial scattering coefficient of the j-th sphere
A	Vector Translation Coefficient
b_n	Mie coefficient
b_{mn}^j	Partial scattering coefficient of the j-th sphere
B	Vector translation coefficient
c_N	Number volume concentration
c_{mn}^j	Expansion coefficient of internal field for j-th sphere
C_{ext}	Extinction cross section
C_{sca}	Scattering cross section
d	Center-to-Center distance
d_{mn}^j	Expansion coefficient of internal field for j-th sphere
E	Extinction
E_{mn}	Normalization factor for field expansions
E_0	Electric field intensity
$\mathbf{E}$	Electric field vector
i	Imaginary unit
I	Intensity
I_0	Incident intensity
$\mathbf{i}$	Unit vector
k	Wave number
l_p	Optical path length
m	Counting variable
$\mathbf{M}_{mn}^{(J)}$	Spherical vector wave function
n	counting variable
N_{prim}	Number of primary particles in agglomerate
N_w	Wiscombe number
$\mathbf{N}_{mn}^{(J)}$	Spherical vector wave function

p_{mn}^{j}	Incident field expansion coefficient for j-th sphere
P_{n}^{m}	Associated Legendre Polynomial
q_{mn}^{j}	Incident field expansion coefficient for j-th sphere
Q_{ext}	Extinction efficiency
T	Transmission
x	Particle size
$z_{n}^{(J)}$	General symbol for spherical Bessel functions of n-th order and J-th kind
α	Size parameter
λ	wavelength in media
π_{mn}	Mie angular function
τ_{mn}	Mie angular function

9 References

[1] B. Wessely, J. Altmann, R. Paluch, S. Ripperger, Proceedings PARTEC 2001, Nürnberg, (2001)

[2] C. Bacon, L. Garcio-Rubio. Proc. Part. Technol. Forum. American Institute of Chemical Engineers Washington D.C. (1998) 717

[3] R. Dittmann, H.-J. Feld, W. Samenfink, S. Wittig. Preprints PARTEC 2 (1992) 507

[4] G. Mie, Ann. Phys. 4. Folge Band 25 (1908) 377

[5] H.C. van de Hulst, Light scattering by small particles; Dover Publications Inc., New York, 1981

[6] M. Kerker, The Scattering of Light and other Electromagnetic Radiation, Academic Press Inc., New York, 1969

[7] C.G. Bohren, D.R. Huffman, Absorption and Scattering of Light by Small Particles; Wiley Publications, New York, 1981

[8] W. Trinks, Ann. Phys. 5. Folge Band 22 (1935) 561

[9] L.L. Foldy, Phys. Rev. 67/3-4 (1945) 107

[10] A.L. Aden, M. Kerker, J. Appl. Phys. 22 (1951) 1242

[11] P.C. Waterman, R. Truell,. J. Math. Phys. 2/4 (1961) 512

[12] O. Asano, G. Yamamoto, Appl. Opt. 14 (1975) 29

[13] P.C. Waterman, Proc. IEEE 53 (1965) 803

[14] A. Doicu, T. Wriedt, J. Modern Opt. 45 (1998) 199

[15] T. Wriedt, Part. Part. Syst. Charact. 15 (1998**)** 67

[16] M.I. Mishchenko, J. Opt. Soc. Am. A 8 (1991) 871

[17] N.G. Khlebtsov, Appl. Opt. 31 (1992) 5359

[18] A.C. Ludwig, Comp. Phys. Comm. 68 (1991) 306

[19] M.I. Mishchenko, L.D. Travis, D.W. Mackowski, J. Quant. Spectrosc. Radiat. Transfer 55 (1996) 535

[20] M.I. Mishchenko, L.D. Travis, A.A. Lacis, Scattering, Absorption and Emission of Light by Small Particles, Cambridge University Press, Cambridge, 2002

[21] J.H. Bruning, Multiple Scattering by Spheres, Ph.D. Thesis, Dep. of Electrical Engineering, University of Illinois, 1969

[22] J.H. Bruning, Y.T. Lo, IEEE Trans. Ant. Prop. AP-19 (1971) 378

[23] J.H. Bruning, Y.T. Lo, IEEE Trans. Ant. Prop. AP-19 (1971) 391

[24] K.A. Fuller, G.W. Kattawar, Opt. Lett. 13/2 (1988) 90

[25] K.A. Fuller, G.W. Kattawar, Opt. Lett. 13/12 (1988) 1063

[26] D.W. Mackowski, Proc. Roy. Soc. London A 433 (1991) 599

[27] Y. Xu, Appl. Opt. 34/21 (1995**)** 4573

[28] Y. Xu, Appl. Opt. 36/36 (1997**)** 9496

[29] Y. Xu, Phys. Lett. A 249 (1998**)** 30

[30] Y. Xu, N.G. Khlebtsov, J. Quant. Spectrosc. Radiat. Transfer 79-80 (2003**)** 1121

[31] O.R. Cruzan, Q. Appl. Math. 20 (1962**)** 33

[32] Y. Xu, J. Comp. Phys. 139 (1998**)** 137

[33] W.J. Wiscombe, Appl. Opt. 19 (1980**)** 1505

[34] Y. Xu, B.Å.S. Gustafson, J. Quant. Spectrosc. Radiat. Transfer 70 (2001**)** 395

[35] Y. Xu, B.Å.S. Gustafson, Appl. Opt. 36/30 (1997) 8026

[36] U. Kätzel, T. Detloff, S. Ripperger, Filtrieren und Separieren 18/1 (2004) 16

[37] B. Wessely, *Extinktionsmessung von Licht zur Charakterisierung disperser Systeme;* Fortschritt-Berichte VDI, Reihe 8, No. 773, VDI Verlag, Düsseldorf, 1998

[38] F. Gruy, J. Colloid Interface Sci. 237 (2001**)**, 28

10 Legend of Illustrations

figure 1: Computation results for Extinction cross sections with interactions (Xu) compared to the Mie case (left: Large size parameters; right: Small size parameters)

figure 2: Scanning Electron Microscopy Image of Agglomerates of Geltech 500 obtained by the Spray Dryer Method

figure 3: Scheme of the Aerosol Resuspension Method for the production of rigid agglomerates

figure 4: Scanning Electron Microscopy Image of Agglomerates of Geltech 500 obtained by the Aerosol Resuspension Method with different particle concentrations in the feed suspension (left : 2 vol.-%; right: 0,47 vol.-%)

figure 5: Volume density distributions of agglomerated Geltech 500 created by Aerosol Resuspension. Stability test by different sonifications marked in the diagram.

figure 6: Different morphologies of Geltech agglomerates in fractionated suspensions: doublet, triplet (60°), triplet (120°), triplet chain and quadruplet (from upper left to lower right)

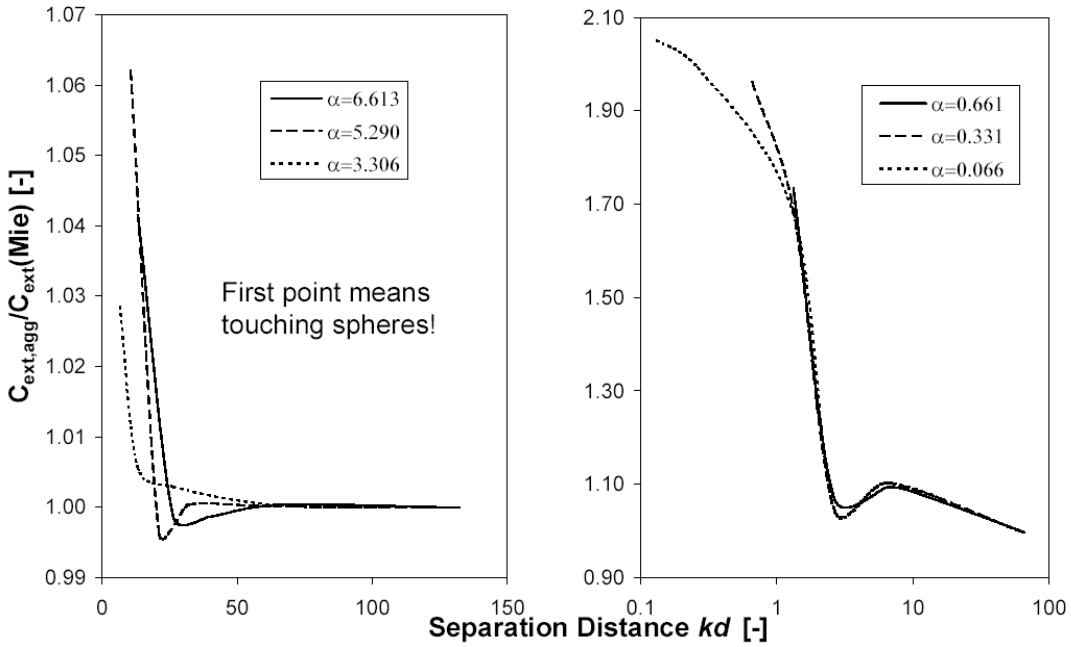

figure 1: Computation results for Extinction cross sections with interactions (Xu) compared to the Mie case (left: Large size parameters; right: Small size parameters)

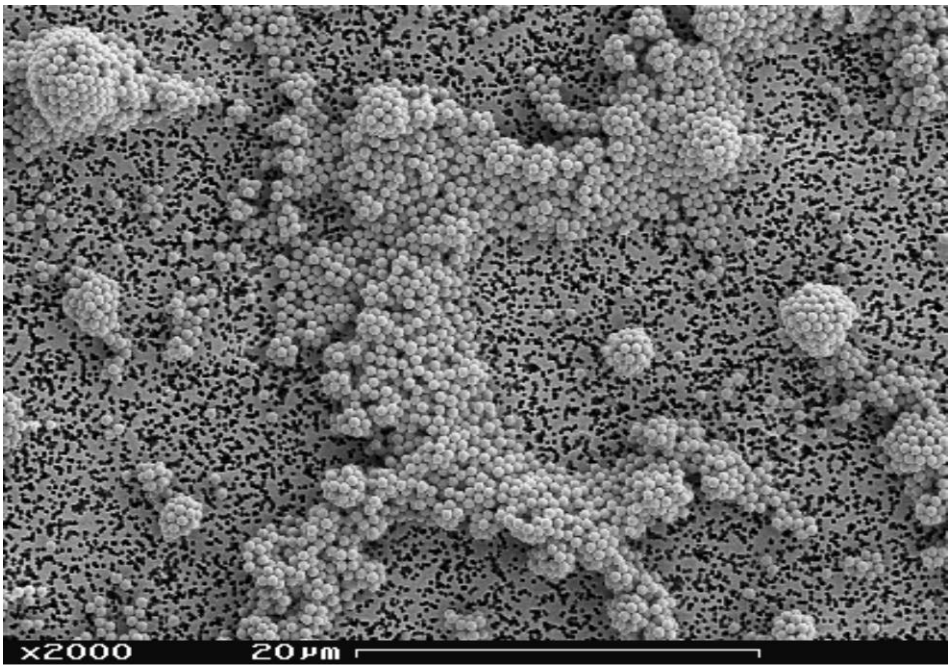

figure 2: Scanning Electron Microscopy Image of Agglomerates of Geltech 500 obtained by the Spray Dryer Method

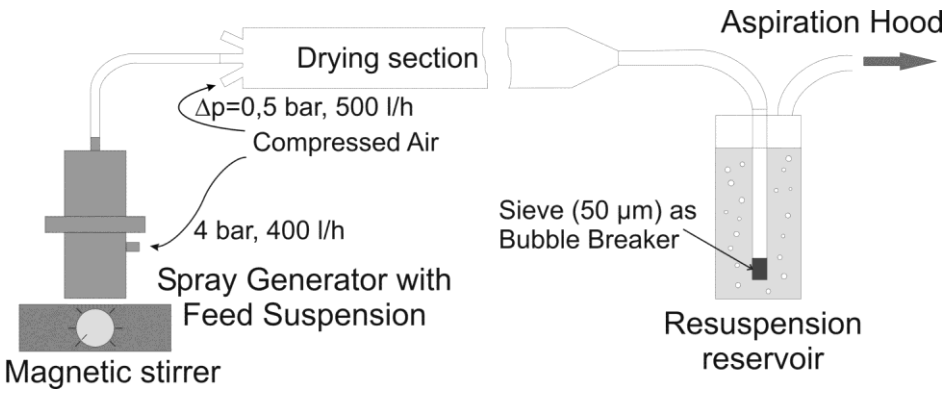

figure 3: Scheme of the Aerosol Resuspension Method for the production of rigid agglomerates

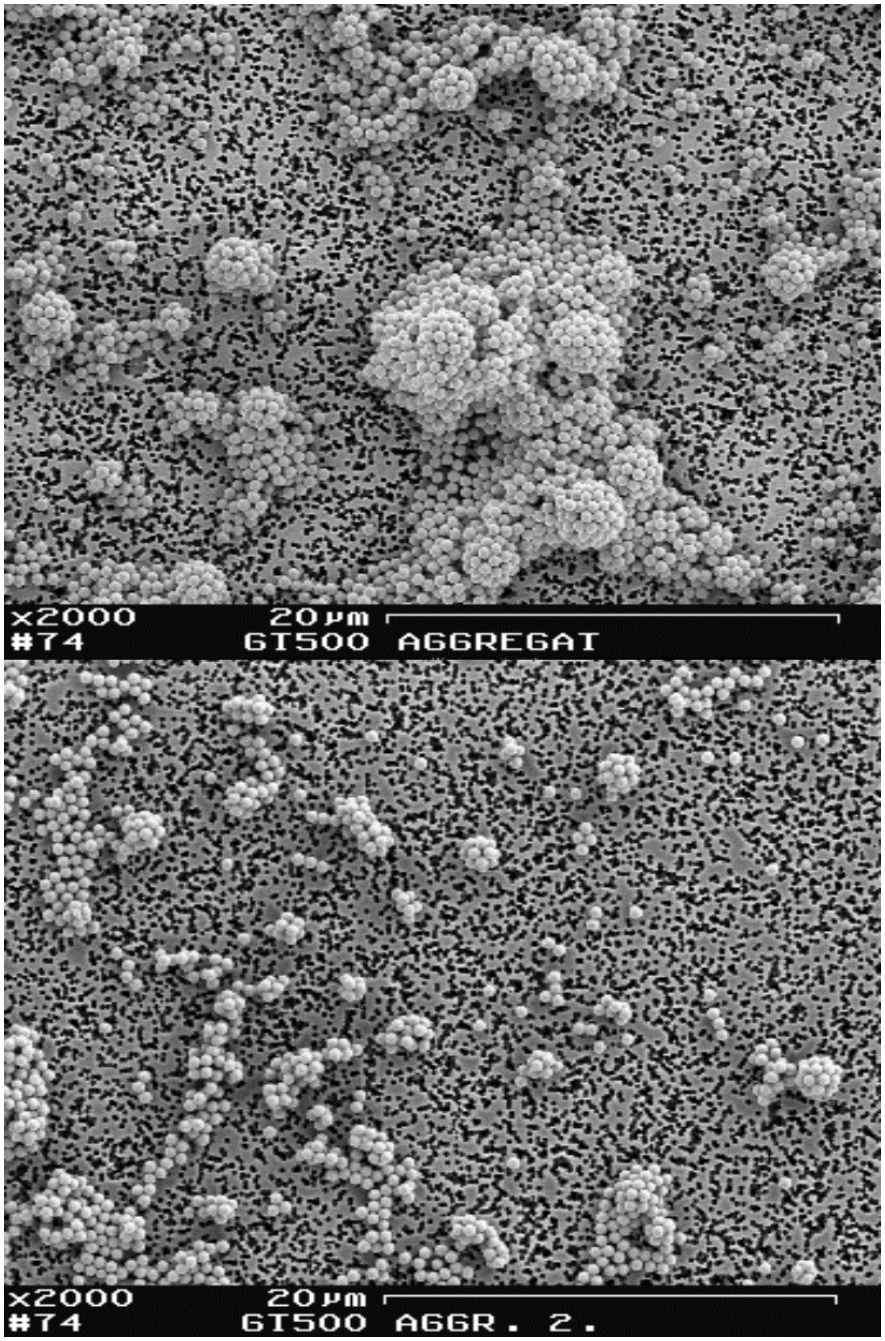

figure 4: Scanning Electron Microscopy Image of Agglomerates of Geltech 500 obtained by the Aerosol Resuspension Method with different particle concentrations in the feed suspension (left : 2 vol.-%; right: 0,47 vol.-%)

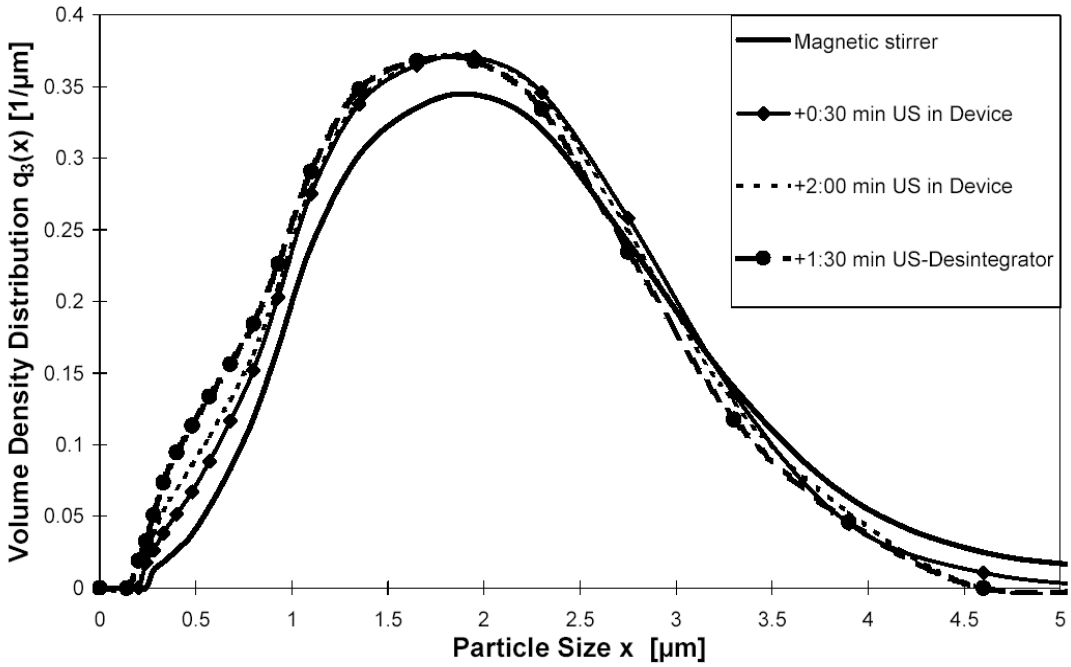

figure 5: Volume density distributions of agglomerated Geltech 500 created by Aerosol Re-suspension. Stability test by different sonifications marked in the diagram.

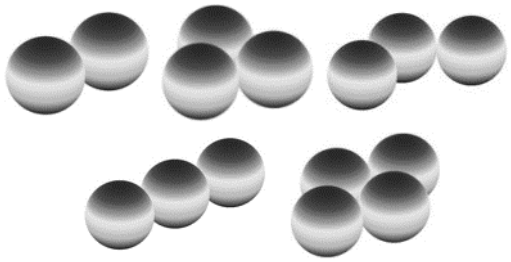

figure 6: Different morphologies of Geltech agglomerates in fractionated suspensions: doublet, triplet (60°), triplet (120°), triplet chain and quadruplet (from upper left to lower right)

11 Tables

Table 1: Refractive Indices for Silica Geltech 500 and Geltech 1000 measured by embedding methods and extinction measurements

Table 2: Relative occurrence of different agglomerate types in the fractionated suspensions of Geltech 500 and Geltech 1000. Counting Results from SEM pictures.

Table 3: Concentrations of the fractionated agglomerate suspensions

Table 4: Comparison of computed and measured volume specific extinction cross sections for the agglomerate suspensions of Geltech 500 and Geltech 1000 at different wavelengths, computed values for suspensions of primary particles are additionally given for comparison

Table 1: Refractive Indices for Silica Geltech 500 and Geltech 1000 measured by embedding methods and extinction measurements

Wavelength [nm]	Geltech 500	Geltech 1000
670	1.432-0.0077i	1.452-0.0012i
875	1.431-0.0050i	1.451-0.0000i

Table 2: Relative occurrence of different agglomerate types in the fractionated suspensions of Geltech 500 and Geltech 1000. Counting Results from SEM pictures.

Agglomerate Type	Relative Frequency	
	Geltech 500	Geltech 1000
Primary Particles	0.733	0.790
Doublets	0.211	0.158
Triplets (60°)	0.023	0.024
Triplets (120°)	0.034	0.021
Triplet Chain	0.000	0.003
Quadruplets	0.000	0.003

Table 3: Concentrations of the fractionated agglomerate suspensions

Silica Type	Concentration [vol.-%]
Geltech 500	0.146
Geltech 1000	0.254

Table 4: Comparison of computed and measured volume specific extinction cross sections for the agglomerate suspensions of Geltech 500 and Geltech 1000 at different wavelengths, computed values for suspensions of primary particles are additionally given for comparison

Wavelength [nm]	Silica Type	$C_{V,ext,agg}$ (comp.) [μm^{-1}]	$C_{V,ext,agg}$ (meas.) [μm^{-1}]	Rel. Deviation [%]	$C_{V,ext,prim}$ (comp.) [μm^{-1}]
670	Geltech 500	0.517	0.554	7.0	0.489
875	Geltech 500	0.276	0.286	3.3	0.257
670	Geltech 1000	0.786	0.787	0.2	0.738
875	Geltech 1000	0.432	0.425	1.5	0.386